TEKSTİL VE KONFEKSİYON

VOL: 34, NO. 3
DOI: 10.32710/tekstilvekonfeksiyon.1284898

Morphological and Mechanical Assessment of Electrospun PLGA Vascular Scaffolds

Suzan Özdemir 0000-0001-7369-2907
Janset Öztemur 0000-0002-7727-9172
Hande Sezgin 0000-0002-2671-2175
İpek Yalçın Enis 0000-0002-7215-3546

Istanbul Technical University / Textile Engineering Department / Istanbul, Turkiye

Corresponding Author: Suzan Özdemir, ozdemirsu@itu.edu.tr

ABSTRACT

Cardiovascular disorders are the leading cause of global mortality and necessitate bypass surgery to replace the damaged blood vessels. Currently used grafts are insufficient to replace small-diameter blood vessels due to the scarcity and harsh harvesting procedures of autologous vessels and the shortcomings in the clinical performance of synthetic grafts. Therefore, there is a critical need for tissue-engineered vascular grafts that can meet morphological, mechanical, and biological characteristics. In this study, poly(lactic-co-glycolic acid) tubular scaffolds with randomly distributed or radially oriented fibers were produced by electrospinning, and the effect of fiber orientation on morphological, physical, and mechanical properties was investigated. Also, instrumental assessments were conducted to perform a comprehensive analysis of the polymeric material, encompassing evaluations of its toxicity and thermal properties. The findings demonstrate that, while successful implementation of radial fiber orientation with high rotational speed production enhanced burst strength and radial tensile strength values, it was unfavorable for compliance.

ARTICLE HISTORY
Received: 19.04.2023
Accepted: 09.11.2023

KEYWORDS

Tissue engineering, Vascular grafts, Compliance mismatch, PLGA

1. INTRODUCTION

Tissue engineering confronts a significant problem in replicating the particular architecture and mechanical properties of the arterial wall in order to meet the basic requirements of the native vessels with diameters smaller than 6 mm [1, 2]. The commonly employed synthetic materials in commercial applications include expanded polytetrafluoroethylene (ePTFE, Gore-Tex) and polyethylene terephthalate (PET, Dacron) [3]. These materials have demonstrated successful outcomes as substitutes for large-caliber arterial grafts like the carotid or common femoral artery, exhibiting favorable long-term results. However, their usage is limited to smaller diameter vascular grafts (< 6mm), such as coronary arteries, due to observed challenges such as poor patency rates resulting from neointimal hyperplasia in peri-anastomotic regions, as well as concerns related to thrombogenicity and compliance mismatch [4, 5]. An efficient vascular graft ought to possess a suitable topology, be biocompatible, antithrombogenic, bioactive, have good mechanical characteristics, and instantly adapt to the existing hemodynamic environment [6]. The mechanical characteristics of vascular prostheses influence biological activities such as the growth of smooth muscle and endothelial cells and accelerate extracellular matrix (ECM) synthesis via enhanced macrophage activity [7]. The ECM deposition is crucial as it is a three-dimensional (3D) network of molecules that provides structural and biochemical support for cells and promotes cell survival, adhesion, proliferation, communication, and differentiation, playing a vital role in cellular processes [8]. Thus, vascular grafts with inadequate mechanical characteristics create an unfavorable microenvironment for neotissue formation [7]. Through the technique of electrospinning, it is feasible to fabricate fibers using biopolymers that closely resemble the complex 3D microenvironment of the ECM. This approach allows for the control and manipulation of various fiber characteristics, such as morphology, diameter, orientation, porosity, pore size, wall thickness, and the creation of multilayered structures [9, 10]. These capabilities enable the replication of the distinct layers present in native blood

To cite this article: Özdemir S, Öztemur J, Sezgin H, Yalçın Eniş İ. 2024. Morphological and mechanical assessment of electrospun plga vascular scaffolds. *Tekstil ve Konfeksiyon*, 34(3), 222-230.

vessels, including the *tunica intima*, *media*, and *adventitia* [9]. The design criteria that affect the properties of vascular grafts can be categorized under two topics: material selection and constructional components such as fiber diameter, pore size, fiber orientation, and wall thickness [11]. For instance, fiber alignment influences how cells grow, how they build their morphologies on scaffolds, and how they align through the vessel wall. Moreover, radial fiber orientation is known to have a beneficial impact on the values of modulus, tensile strength in the same direction, and burst strength, whereas it reduces compliance [12]. On the other hand, excessive wall thickness within the vascular scaffolds creates a disadvantageous situation in terms of cell activities and proliferation, as it restricts features such as porosity and compliance [13]. Compliance, expressed as a percentage of diameter change per 100 mmHg, serves as a measure of flexibility or stiffness [14]. The mismatch in compliance between a rigid vascular graft and the native vessel at the anastomosis sites can lead to issues such as turbulent blood flow and reduced blood flow rates in small grafts. This, combined with the thrombogenic nature of foreign materials used in the graft and the absence of endothelialization, contributes to thrombosis and narrowing of the blood vessel (luminal constriction) due to intimal hyperplasia. Consequently, these factors result in poor graft patency rates [15]. Also, the choice of biomaterials is critical in establishing the framework for mechanical qualities, cellular activities, biocompatibility, biodegradability, and anti-toxicity [16]. In this regard, poly(lactic-co-glycolic acid) (PLGA) is a synthetic biopolymer which supports the biological activities and has tunable mechanical strength and biodegradation rate [17]. Malik et al. (2021), produced tubular fibrous scaffolds with oriented fibers consisting of various biopolymers such as PLGA, polycaprolactone (PCL) and polyvinyl acetate (PVA). PLGA vascular grafts outperformed other polymers in terms of tensile strength (9.1 ± 0.6 MPa), suture retention strength, and burst pressure (350 ± 50 mmHg). These scaffolds have also been discovered to have appropriate porosity and elongation characteristics (87% and 183%, respectively), making them viable materials for vascular grafts. When the aligned scaffolds were compared with their counterparts, remarkable improvements in the mechanical properties such as tensile strength, strain, and burst strength were observed in all the samples (2 MPa vs. 9.1 MPa, 120% vs. 183%, and 350 mmHg vs. 680 mmHg, respectively, for PLGA) [18]. In another study of Johnson et al. (2015) the effect of polymer selection and wall thickness on the mechanical features of the vascular prosthesis was investigated. First of all, the biomechanical characteristics of electrospun vascular grafts made of various biopolymers were examined. The bursting strength of the scaffold made of PLGA showed the highest value with 3.3 MPa, which is slightly higher than the burst pressure of commercially used Dacron graft with 3.2 MPa. However, compliance results revealed that PLGA grafts demonstrate a relatively low compliance value of 1.9%/mmHg [19].

Within the scope of this study, electrospun vascular prostheses consisting of randomly distributed and radially oriented PLGA fibers were fabricated for the purpose of assessing both the effect of fiber arrangement on the mechanical properties in terms of tensile strength and strain, burst strength, and compliance, as well as determining the suitability of PLGA scaffolds in regards to physical, morphological, chemical, thermal, and mechanical characteristics.

2. MATERIAL AND METHOD

2.1 Material

PLGA (Mw: 50,000–75,000 g/mol, PLA/PGA:85/15) was used as a polymer, whereas chloroform (CH), acetic acid (AA), and ethanol (ETH) were utilized as the solvent system components. The chemicals were purchased from Sigma-Aldrich.

2.2 Method

Fabrication of PLGA vascular grafts

PLGA was dissolved in CHL/ETH/AA (8/1/1 wt.) at a concentration of 18% wt. based on preliminary studies [20]. The tubular samples were produced using an electrospinning unit (Nanospinner, Ne100+) provided by Inovenso, Turkey. The PLGA solutions were delivered by using a feeding rate of 2.25 ± 0.25 ml/h and subjected to 11 ± 2 kV voltage by using 20 cm needle to collector distance. Rotating rod collectors with 5 mm diameter and different rotational speeds of 200 rpm and 10,000 rpm were used to achieve samples with randomly distributed (PLGA_R) and radially oriented fibers (PLGA_O). The spinning time for all samples was set at 40 minutes to achieve the adequate wall thickness expected from vascular grafts.

Morphological and physical characterization

SEM Analysis

The surface morphologies of electrospun surfaces were investigated by using a scanning electron microscope (SEM). The SEM images of tubular scaffolds were taken with magnifications of 1kx.

Fiber diameter and wall thickness measurement

The Image J Software System was used to calculate average fiber diameters from SEM images of at least 50 distinct fibers. The wall thickness of samples was measured with a Standard Gage Electronic External Micrometer (Hexagon Metrology, Turkey).

Water contact angle assessment

The KSV Attension Optical Contact Angle Meter is employed to measure the water contact angles on scaffold

surfaces using the sessile drop measurement technique, enabling the evaluation of surface hydrophilicity. The contact angle serves as a valuable indicator, conveying insights into surface hydrophilicity and wettability. A higher contact angle on the surface corresponds to reduced hydrophilicity and wettability [21].

Chemical and thermal characterization

Fourier-transform infrared spectroscopy analysis (FTIR)

FTIR analysis was conducted employing Fourier-transform infrared spectrometry (UATR Two, Perkin Elmer) to detect the presence of characteristics peaks of PLGA. This analysis also serves to substantiate the absence of any residual solvents within the fibrous scaffolds subsequent to their production. The infrared absorption spectra of the samples were obtained within the range of 500–4000 cm^{-1}.

Differential scanning calorimetry (DSC) analysis

The Perkin Elmer DSC400 was used to conduct the thermal analysis and also the confirm the amorphous structure of the PLGA webs. The analysis took place under atmospheric pressure in a nitrogen atmosphere, with a sample weight of 5 mg. The PLGA webs were subjected to a heating rate of 7°C/min, starting from 30°C and reaching a maximum temperature of 400°C. By measuring the heat flow during the temperature ramp, the DSC provides valuable data for determining both the glass transition temperature (T_g) and the maximum decomposition rate of the PLGA webs [22, 23].

Mechanical assessment

Tensile strength and strain

Tensile testing was performed by using Zwick-Roell Z005 universal testing machine (ZwickRoell, Germany) for the assessment of the mechanical performance of the tubular grafts. The tubular samples were tested in axial (0°) and radial (90°) directions in both planar (_P) and tubular form (_T). The planar test samples were cut into 10mm x 15mm (width x length) dimensions from tubular scaffolds whereas tubular samples with 1.5 cm length were cut for testing in tubular manner. Testing the samples in tubular shape along the longitudinal direction arises from simulating the position of vascular grafts in the body and examining how they respond to mechanical forces in its own shape. The cross-head speed was set at 10 mm/min while the distance between the gauges was 5 mm.

Burst pressure measurement

The burst strength measurement is utilized to assess the maximum pressure that a vascular prosthesis can endure before experiencing failure [24]. The burst pressure properties of the tubular graft structures were measured by custom design burst tester (Inovenso, Turkey). The balloon was placed into the tubular samples cut in 4 cm length. Then, the sample ends were fastened into the air nozzles with the help of sleeves, and pressurized air flow was provided. The burst pressure value was recorded when the sample fails as a result of supplied air pressure from the nozzles.

Compliance

The custom-designed device (Inovenso, Turkey) with provided air flow used to measure the compliance at a physiologically equivalent pressure of 80–120 mmHg as specified in ISO 7198:2016 [25]. The photographs of the samples under provided pressure ranges were captured using a camera system. The Image J software system was then utilized to measure the diameters of the samples at each pressure. Then, the compliance values were calculated by the formula given in Equation (1).

$$\%compliance = \frac{\frac{Rp_2 - Rp_1}{Rp_1}}{p_2 - p_1} \times 10^4 \quad \text{Eq. 1}$$

where R_{p2} is a pressurized radius at diastolic pressure (mm), R_{p1} is a pressurized radius at systolic pressure (mm), p_1 is a diastolic pressure (mmHg), and p_2 is a systolic pressure (mmHg). To ensure accuracy and reliability, compliance measurements for each vascular graft were repeated a minimum of three times

3. RESULTS AND DISCUSSION

3.1 SEM analysis

SEM images, which are represented in Figure 1, revealed that both scaffolds consist of smooth, homogenous, and bead-free fibers. In the research conducted by Stojko et al. (2020), electrospun wound dressings with PLGA consisting of different proportions of lactic acid (LA) and glycolic acid (GA) (50/50, 70/30, and 85/15) was produced by using chloroform based solvent system and polymer concentrations of 15-18% wt. SEM examinations showed that the resulting fibers exhibited a consistent, elongated, and smooth structure [26]. On the other hand, the radial fiber orientation was achieved when the collector speed was set at 10,000 rpm. The high collector speed causes a higher linear velocity of the mandrel, which supports the fiber alignment in the circumferential direction [27]. The attainment of randomly distributed fibers on the collector can be accomplished by adjusting the rotational speed to a value below the take-up speed of the fibers. This ensures that the fibers are not aligned in a specific orientation, leading to a random arrangement on the collector surface [28]. Hu et al. (2012) also produced vascular grafts with electrospun PCL fibers, achieving various fiber orientations by altering the collector's rotation speed. Through optical microscopy, they determined that faster collector rotation resulted in higher degree of fiber alignment [29].

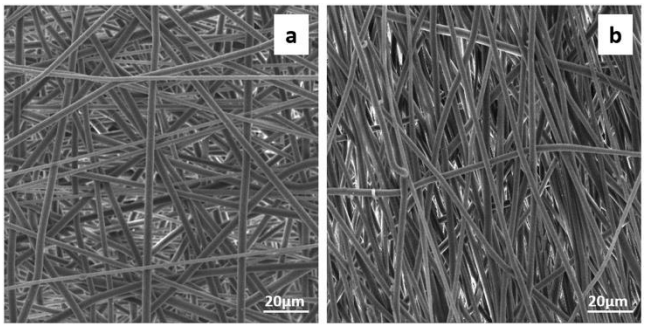

Figure 1. SEM images at 1kx magnification of neat PLGA samples produced on tubular collector with rotational speeds of 200 rpm and 10,000 rpm (a) PLGA_R and (b) PLGA_O.

3.2 Fiber diameter and wall thickness measurement

The fiber diameters of the produced scaffolds, as presented in Table 1, range between 2.3 and 2.6 µm. Fiber diameters are affected by many parameters in electrospinning, such as voltage, solvent systems, polymer concentration, flow rate, spinneret diameter, rotational speed, and so on [30, 31]. In a study of Milleret et al. (2012), PLGA vascular grafts were manufactured by employing chloroform as a solvent and modifying electrospinning parameters. They measured fiber diameters, which spanned from 0.63 µm to 5.02 µm, contingent upon the chosen parameters [32]. Similarly, Ko et al. (2016) generated electrospun PLGA surfaces using various solvents, resulting in fiber diameters ranging between 0.2 µm and 5 µm. Notably, surfaces produced with chloroform exhibited the largest fiber diameter at 5 µm [33]. In a separate study, You et al. (2005) examined the fiber diameters of samples produced from polyglycolic acid (PGA), polylactic acid (PLA), and PLGA. PLGA exhibited thicker fiber diameters, ranging from 0.2 to 1.8 µm. This variation was attributed to solvent properties, including electrical conductivity and polarity [34]. Existing literature highlights that the use of non-polar solvents like chloroform or dichloromethane leads to an increase in fiber diameters [35]. Also, it can be seen from the fiber diameter values that the PLGA_O sample has thinner fibers than the PLGA_R sample. This situation can be explained by the stretching of the fibers because of the rotational movement and speed of the rotating collector [36, 37]. Fibrous webs generated at higher rotational speeds result in thinner fiber diameters compared to those produced at lower collector speeds due to the application of stretching force [38]. On the other hand, the wall thickness values measured in both grafts are sufficient and fall within the wall thickness range given for vascular grafts in the literature (200 µm-600 µm) [39]. It is also emphasized that the wall thickness of the vascular grafts should be as thin as possible if they can demonstrate enough mechanical endurance and biodegradation [40]. In the current investigation, despite employing identical production systems and durations, variations in wall thickness were observed, particularly in relation to different collector rotation speeds. This suggests that the collector speed can influence the wall thickness of the produced fibers. It is hypothesized that a high-speed rotating collector rapidly draws in the fibers, limiting their dispersion and resulting in a thicker wall structure.

Table 1. Wall thicknesses, fiber diameters, and fiber diameter histograms of PLGA vascular grafts.

Samples	Wall thickness (µm)	Fiber diameter (µm)	Fiber diameter distribution
PLGA_R	208 ± 33	2.579 ± 0.782	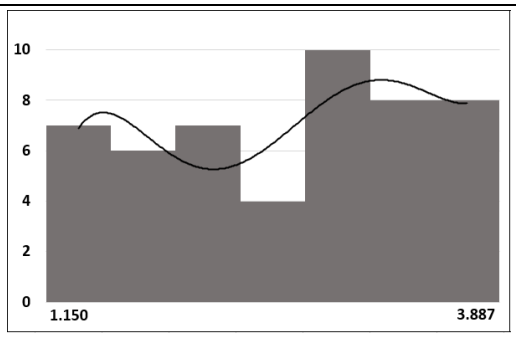
PLGA_O	245 ± 28	2.372 ± 0.407	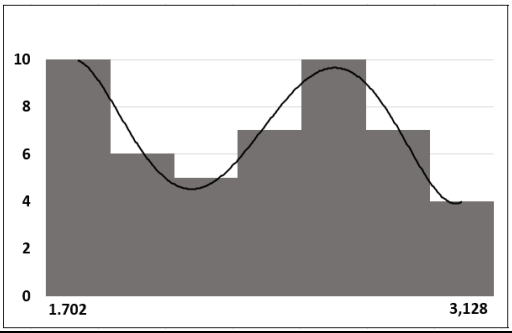

3.3 Analysis of surface wetting properties

Table 2 displays the water contact angles observed on the PLGA scaffolds. Both samples exhibit hydrophobic characteristics, as indicated by their relatively high contact angles, impacting the surfaces' wettability. Notably, there isn't a substantial difference between the contact angles of the two samples. Furthermore, it's worth mentioning that the contact angle and surface hydrophilicity aren't linked to the orientation of the fibers but are instead related to the nature of the polymer itself. This aligns with the expected hydrophobic behavior of PLGA, as supported by prior research [41, 42], which can be attributed to the high content of lactic acid within the polymer (85%). The existence of methyl side groups in lactic acid increases its hydrophobicity compared to glycolic acid. As a result, copolymers of PLGA rich in lactide are less prone to absorbing water due to their reduced hydrophilicity, which leads to a slower degradation process [43]. In a study of Ji Lee et al. (2014), the fibrous webs consisting of neat PLGA showed a hydrophobic character with a water contact angle of 143° [44]. As it is widely recognized that increased hydrophilicity enhances surface polarity and adhesion, facilitating cell attachment and proliferation [45], existing experimental studies also demonstrate that cells can adhere to and thrive on PLGA surfaces characterized by high contact angles [46, 47].

3.4 FTIR analysis

Figure 2 confirms the presence of characteristic peaks in the PLGA fibrous webs. Analysis of the FTIR spectra reveals prominent features in specific wavenumber ranges. A distinct broad band between 1700 cm^{-1} and 1800 cm^{-1}, corresponding to the carbonyl (C=O) groups present in both monomers, is observed [48]. Additionally, a grouping band (C-O) between 1300 cm^{-1} and 1150 cm^{-1}, indicative of ester groups, is evident [49]. Moreover, the spectrum clearly exhibits stretching vibrations of the CH, CH_2, and CH_3 groups (2850–3000 cm^{-1}) [50]. Notably, the absence of characteristic peaks from chloroform, ethanol, and acetic acid in the FTIR analysis indicates the absence of residue from these solvents on the fibrous webs. Specifically, chloroform, the primary solvent, does not exhibit its characteristic peaks, including CCl_3 stretching at 680 and 774 cm^{-1}, and C-H stretching at 3034 cm^{-1} [51]. Similarly, ethanol, with its characteristic peaks of C-O stretching at 2055 cm^{-1}, symmetric CH stretching at 2850 cm^{-1}, and asymmetric C-H stretching at 2850 cm^{-1}, was not observed in the PLGA sample [45]. Likewise, acetic acid, with its peaks of C-O and OH vibrations at 1292 cm^{-1}, and C-H vibrations at 1424 cm^{-1}, was not detected in the FTIR spectra of PLGA webs [52]. FTIR analysis conducted in preliminary studies further substantiated the absence of chloroform, ethanol, and acetic acid on the fibrous web [45, 53].

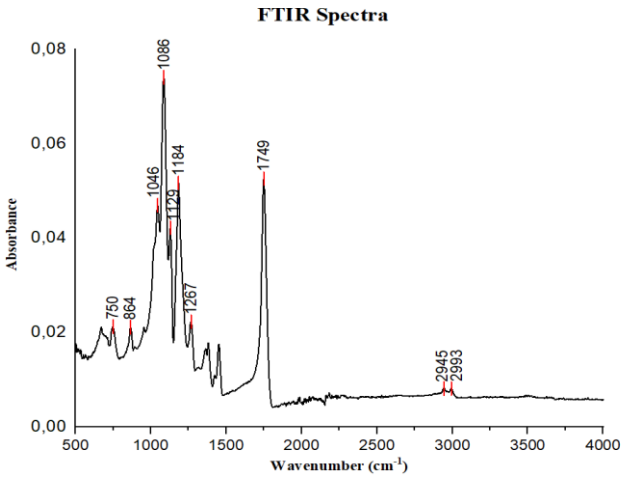

Figure 2. FTIR Spectra of PLGA web

3.5 DSC analysis

The results of the differential scanning calorimetry (DSC) performed on pure PLGA webs is displayed in Figure 3. Thermal and chemical analyses were conducted on both scaffolds, but the results are given in single curves since it is observed that the rotational speed does not have a significant impact on the thermal and chemical properties of the produced webs, which is also supported by existing literature [54]. The DSC analysis revealed an endothermic event at 52.9°C, indicating a thermal transition within the material. Additionally, an endothermic decomposition peak was observed, which centered around 334.4°C. The obtained results are consistent with previous findings reported in the literature [55, 56, 57]. The glass transition temperature of PLGA is higher than the physiological temperature, indicating that the mobility and elasticity of the polymeric material are low and that the material shows brittle behavior within the human body [58, 59]. It is also important to note that since the PLGA used in this study is in an amorphous form, it does not exhibit a melting point. Melting behavior is characteristic of polymers with a semi-crystalline structure, whereas amorphous polymers lack the ordered arrangement necessary for melting to occur [60]. Therefore, the absence of a melting point in the DSC spectra supports the amorphous nature of the PLGA utilized in this study.

Table 2. Contact angle measurements of the PLGA scaffolds.

Samples	Contact Angle Mean (°)	Water Droplet Image
PLGA_R	137.12 ± 0.64	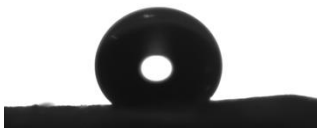
PLGA_O	138.30 ± 0.64	

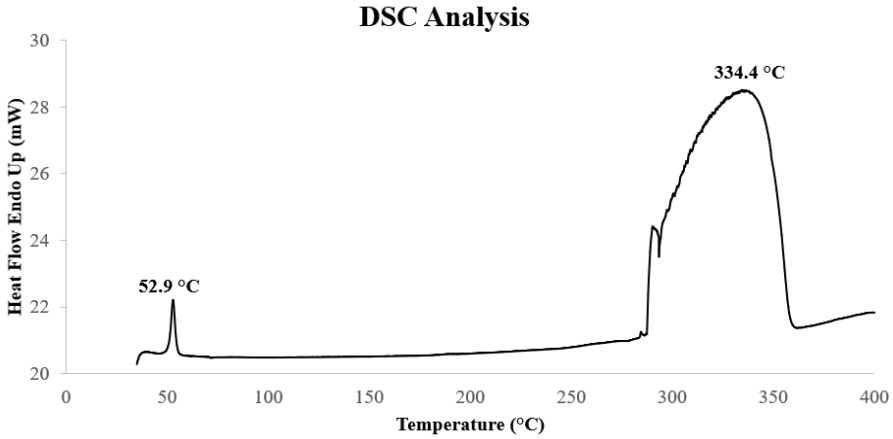

Figure 3. DSC curve of PLGA

3.6 Tensile strength and elongation

When the tensile strength and strain values (Table 3) are investigated, it has been seen that the radial fiber orientation contributed to the strength values in the radial direction with an increment from 3.81 MPa to 6.23 MPa, whereas it caused a decrement in the tensile strength values in the longitudinal direction as the fibers were all aligned in the radial direction, which enabled them to resist the applied stress collectively [61]. The findings of Wu et al. (2010) offer further support to the aforementioned observation. In their study on PCL vascular grafts, they manipulated the electrical field and adjusted the rotational speeds to generate grafts with either radial or axial fiber orientations. Their results demonstrated a notable reduction in strength along the axial direction in the radially oriented scaffolds, indicating the fibers' inability to withstand the applied load in that axial orientation [62]. On the other hand, the elongation values were improved in all directions with radial fiber orientation. In a study conducted by Malik et al. (2021), when the tensile testing results of the scaffolds with oriented and non-oriented PLGA fibers are compared, it was found that the tensile strength values for non-oriented scaffolds are lower, and the strain values are also lower. It is reported that the PLGA scaffolds with randomly distributed fibers have a tensile strength and strain of around 2 MPa and 125%, while the ones with oriented fibers have a tensile strength of 9.1 MPa and 150% [18]. In addition, the strain value of PLGA_O in the radial direction was much lower than that in the longitudinal direction because, as the oriented fibers are already under stress in their alignment direction and there are fewer junctions of fibers, they cannot be stretched too much in that direction [63]. Upon conducting a comprehensive examination of the orientation's effect, considering the test direction, it becomes evident that the tensile strength results of PLGA scaffolds with randomly distributed fibers exhibit different mechanical behavior compared with scaffolds with radial fiber orientation. Specifically, the radial (90°) direction demonstrated the lowest tensile strength values of 3.81 MPa, whereas the longitudinal (0°) direction displayed the highest strength values of 4.53 MPa and 5.89 MPa. This phenomenon can be attributed to the greater alignment of fibers in the longitudinal direction, as a consequence of the low rotational speed, which hinders their radial alignment and promotes their accumulation and alignment on the collector surface in the longitudinal direction [38]. The tensile strength and elongation values obtained from the PLGA scaffolds surpassed the literature-reported tensile testing results of the human coronary artery, with axial and radial tensile strengths measuring 1.02 MPa and 1.05 MPa, respectively, and the elongation values ranging from 45% to 99% [64, 65].

3.7 Burst strength and compliance

The burst strength and compliance measurement results are given in Table 4. The values show that the fiber orientation resulted in improved burst strength, whereas it slightly reduced the compliance levels. The orientation of fibers plays a crucial role in controlling compliance and burst pressure of grafts [66]. Aligned fibers, when subjected to strain along their alignment direction, demonstrate increased modulus, tensile strength, and burst pressure values but reduced compliance due to their stiffer structure [63]. Therefore, for an optimal balance between compliance and burst pressure resistance, particularly in the anastomotic region, a multilayer approach using carefully selected fiber orientations is necessary [67]. This approach has been advocated for achieving desired mechanical properties in vascular replacements. This situation is also supported by the study of Grasl et al. (2021), which showed that the burst strength of polylactic acid scaffolds increased from 570 ± 188 mmHg to 7641 ± 902 mmHg with radial fiber orientation, whereas compliance was reduced from 29.7%/100 mmHg to 4.1%/100 mmHg by fiber orientation in the radial direction for the polyurethane samples because of the increased stiffness of the scaffolds [68]. The results showed that the mechanical properties satisfy the minimum limits for the human saphenous vein (1599 mmHg and 0.6-1.5 %/100 mmHg) [69].

Table 3. The tensile strength and strain values of the PLGA planar and tubular samples with randomly distributed and radially oriented fibers.

	Test direction	Tensile Strength (MPa)	Strain (%)		Test direction	Tensile Strength (MPa)	Strain (%)
PLGA_R	0º_P	4.53 ± 0.80	60.41 ± 17.09	**PLGA_O**	0º_P	1.85 ± 0.42	851.01 ± 115.39
	90º_P	3.81 ± 0.07	48.34 ± 5.61		90º_P	6.23 ± 0.42	54.61 ± 20.84
	0º_T	5.89 ± 0.96	116.26 ± 55.85		0º_T	2.89 ± 0.23	1085.39 ± 83.10

Table 4. The burst strength and compliance values of the PLGA tubular samples with randomly distributed and radially oriented fibers.

Samples	Burst Strength (mmHg)	Compliance (%/100 mmHg)
PLGA_R	1873.50 ± 136.47	1.416 ± 0.025
PLGA_O	2889.00 ± 32.53	1.345 ± 0.082

4. CONCLUSION

The morphological analyses provided compelling evidence of successful fibrous surface production. Furthermore, the chemical analysis of the surface revealed the absence of solvent residue, as evident from the lack of characteristic peaks in the FTIR spectra. Notably, the FTIR spectra exhibited distinct characteristic peaks that correspond to PLGA, confirming its presence on the surface. Additionally, the DSC analysis demonstrated that the glass transition temperature of PLGA exceeds the physiological temperature, implying its propensity for exhibiting brittle behavior within the human body and at room temperature. Also, optimizing the design of the PLGA scaffolds by fiber orientation has proven to be a useful solution in regards to mechanical properties. Radial fiber orientation was successfully achieved in the produced fibrous vascular grafts, which also have sufficient wall thickness for mechanical tests. Alignment of the fibers along the periphery of the graft contributed to the tensile strength values in the radial direction and burst strength, resulting in a decrease in the compliance values. At the same time, the difference between the elongation values in the longitudinal and radial directions dramatically increased in the scaffolds with a radial orientation. The overall results showed that the manufactured scaffolds are promising for use in vascular grafts and can mimic the mechanical response of the native blood vessels if the stiffness problem in the radial direction can be eliminated by polymer blending or a multi-layered design approach for taking advantage of more ductile polymers.

Acknowledgement

This study is supported by TUBITAK under grant no. 121M309 and ITU Scientific Research Projects Fund under grant no. 43368 and 44230.

REFERENCES

1. A Nerem, R. M., & Seliktar, D. (2001). Vascular tissue engineering. *Annual Review of Biomedical Engineering*, 3, 225–243. https://doi.org/10.1146/annurev.bioeng.3.1.225
2. Awad, N. K., Niu, H., Ali, U., Morsi, Y. S., & Lin, T. (2018). Electrospun fibrous scaffolds for small-diameter blood vessels: A review. *Membranes* 8(1) https://doi.org/10.3390/membranes8010015
3. Ravi, S., & Chaikof, E. L. (2010). Biomaterials for vascular tissue engineering. In *Regenerative Medicine* (Vol. 5, Issue 1, pp. 107–120). https://doi.org/10.2217/rme.09.77
4. Carrabba, M., & Madeddu, P. (2018). Current strategies for the manufacture of small size tissue engineering vascular grafts. In *Frontiers in Bioengineering and Biotechnology* (Vol. 6, Issue APR). Frontiers Media S.A. https://doi.org/10.3389/fbioe.2018.00041
5. Teebken, O. E., & Haverich, A. (2002). *Tissue Engineering of Small Diameter Vascular Grafts*. http://www.idealibrary.com
6. Obiweluozor, F. O., Emechebe, G. A., Kim, D. W., Cho, H. J., Park, C. H., Kim, C. S., & Jeong, I. S. (2020). Considerations in the Development of Small-Diameter Vascular Graft as an Alternative for Bypass and Reconstructive Surgeries: A Review. *Cardiovascular Engineering and Technology*, 11(5), 495–521. https://doi.org/10.1007/s13239-020-00482-y
7. Zhao, L., Li, X., Yang, L., Sun, L., Mu, S., Zong, H., Li, Q., Wang, F., Song, S., Yang, C., Zhao, C., Chen, H., Zhang, R., Wang, S., Dong, Y., & Zhang, Q. (2021). Evaluation of remodeling and regeneration of electrospun PCL/fibrin vascular grafts *in vivo*. *Materials Science and Engineering C* 118(August 2020). https://doi.org/10.1016/j.msec.2020.111441
8. Safak, S., Vatan, O., Cinkilic, N., & Karaca, E. (2020). In vitro evaluation of electrospun polysaccharide based nanofibrous mats as surgical adhesion barriers. *Tekstil ve Konfeksiyon*, *30*(2), 99–107. https://doi.org/10.32710/tekstilvekonfeksiyon.548460
9. Chen, Y., Dong, X., Shafiq, M., Myles, G., Radacsi, N., & Mo, X. (2022). Recent Advancements on Three-Dimensional Electrospun Nanofiber Scaffolds for Tissue Engineering. In *Advanced Fiber Materials* (Vol. 4, Issue 5, pp. 959–986). Springer. https://doi.org/10.1007/s42765-022-00170-7
10. Sancak, E. , Ozen, M. S. , Erdem, R. , Yılmaz, A. C. , Yuksek, M. , Soın, N. & Shah, T. (2018). PA6/SILVER BLENDS: INVESTIGATION OF MECHANICAL AND ELECTROMAGNETIC SHIELDING BEHAVIOUR OF ELECTROSPUN NANOFIBERS. *Tekstil ve Konfeksiyon*, 28 (3), 229-235. Retrieved from https://dergipark.org.tr/tr/pub/tekstilvekonfeksiyon/issue/39534/466846
11. Yalcin Enis, I., & Gok Sadikoglu, T. (2018). Design parameters for electrospun biodegradable vascular grafts. *Journal of Industrial Textiles* 47 (8), 2205–2227. https://doi.org/10.1177/1528083716654470
12. Ozdemir, S., Yalcin-Enis, I., Yalcinkaya, B., & Yalcinkaya, F. (2022). An Investigation of the Constructional Design Components Affecting the Mechanical Response and Cellular Activity of Electrospun Vascular Grafts. *Membranes* 12(10), 929. https://doi.org/10.3390/membranes12100929

13. Meng, X., Wang, X., Jiang, Y., Zhang, B., Li, K., & Li, Q. (2019). Suture retention strength of P(LLA-CL) tissue-engineered vascular grafts. *RSC Advances* 9(37), 21258–21264. https://doi.org/10.1039/c9ra04529e

14. Pérez-Aranda, C., Gamboa, F., Castillo-Cruz, O., Cauich-Rodríguez, J. v., & Avilés, F. (2019). Design and analysis of a burst strength device for testing vascular grafts. *Review of Scientific Instruments*, *90*(1). https://doi.org/10.1063/1.5037578

15. Hiob, M. A., She, S., Muiznieks, L. D., & Weiss, A. S. (2017). Biomaterials and Modifications in the Development of Small-Diameter Vascular Grafts. *ACS Biomaterials Science and Engineering*, *3*(5), 712–723. https://doi.org/10.1021/acsbiomaterials.6b00220

16. Yu, E., Mi, H. Y., Zhang, J., Thomson, J. A., & Turng, L. S. (2018). Development of biomimetic thermoplastic polyurethane/fibroin small-diameter vascular grafts via a novel electrospinning approach. *Journal of Biomedical Materials Research - Part A* 106(4), 985–996. https://doi.org/10.1002/jbm.a.36297

17. In Jeong, S., Kim, S. Y., Cho, S. K., Chong, M. S., Kim, K. S., Kim, H., Lee, S. B., & Lee, Y. M. (2007). Tissue-engineered vascular grafts composed of marine collagen and PLGA fibers using pulsatile perfusion bioreactors. *Biomaterials* 28(6), 1115–1122. https://doi.org/10.1016/j.biomaterials.2006.10.025

18. Malik, S., Sundarrajan, S., Hussain, T., Nazir, A., & Ramakrishna, S. (2021). Fabrication of highly oriented cylindrical polyacrylonitrile, poly(Lactide-co-glycolide), polycaprolactone and poly(vinyl acetate) nanofibers for vascular graft applications. *Polymers*, *13*(13). https://doi.org/10.3390/polym13132075

19. Johnson, J., Ohst, D., Groehl, T., Hetterscheidt, S., & Jones, M. (2015). Development of Novel, Bioresorbable, Small-Diameter Electrospun Vascular Grafts. *Journal of Tissue Science & Engineering* 6(2). https://doi.org/10.4172/2157-7552.1000151

20. Ozdemir, S. (2023). *INVESTIGATION OF MECHANICAL PROPERTIES OF SMALL CALIBER FIBROUS VASCULAR GRAFTS*. Istanbul Technical University.

21. Kung, C. H., Sow, P. K., Zahiri, B., & Mérida, W. (2019). Assessment and Interpretation of Surface Wettability Based on Sessile Droplet Contact Angle Measurement: Challenges and Opportunities. In *Advanced Materials Interfaces* (Vol. 6, Issue 18). Wiley-VCH Verlag. https://doi.org/10.1002/admi.201900839

22. Miranda, M. I. G., Bica, C. I. D., Nachtigall, S. M. B., Rehman, N., & Rosa, S. M. L. (2013). Kinetical thermal degradation study of maize straw and soybean hull celluloses by simultaneous DSC-TGA and MDSC techniques. *Thermochimica Acta*, *565*, 65–71. https://doi.org/10.1016/j.tca.2013.04.012

23. Rasoulianboroujeni, M., Fahimipour, F., Shah, P., Khoshroo, K., Tahriri, M., Eslami, H., Yadegari, A., Dashtimoghadam, E., & Tayebi, L. (2019). Development of 3D-printed PLGA/TiO 2 nanocomposite scaffolds for bone tissue engineering applications. *Materials Science and Engineering C*, *96*, 105–113. https://doi.org/10.1016/j.msec.2018.10.077

24. Kim, S. H., Mun, C. H., Jung, Y., Kim, S. H., Kim, D. I., & Kim, S. H. (2013). Mechanical properties of compliant double layered poly(L-lactide-co-ε- caprolactone) vascular graft. *Macromolecular Research*, *21*(8), 886–891. https://doi.org/10.1007/s13233-013-1095-5

25. British Standards Institution. (2017). *Cardiovascular implants and extracorporeal systems - vascular prostheses - tubular vascular grafts and vascular patches.* British Standards Institution.

26. Stojko, M., Włodarczyk, J., Sobota, M., Karpeta-Jarząbek, P., Pastusiak, M., Janeczek, H., Dobrzyński, P., Starczynowska, G., Orchel, A., Stojko, J., Batoryna, O., Olczyk, P., Komosińska-Vassev, K., Olczyk, K., & Kasperczyk, J. (2020). Biodegradable electrospun nonwovens releasing propolis as a promising dressing material for burn wound treatment. *Pharmaceutics*, *12*(9), 1–18. https://doi.org/10.3390/pharmaceutics12090883

27. Nitti, P., Gallo, N., Natta, L., Scalera, F., Palazzo, B., Sannino, A., & Gervaso, F. (2018). Influence of nanofiber orientation on morphological and mechanical properties of electrospun chitosan mats. *Journal of Healthcare Engineering* 2018 (November). https://doi.org/10.1155/2018/3651480

28. Baji, A., Mai, Y. W., Wong, S. C., Abtahi, M., & Chen, P. (2010). Electrospinning of polymer nanofibers: Effects on oriented morphology, structures and tensile properties. In *Composites Science and Technology* (Vol. 70, Issue 5, pp. 703–718). Elsevier Ltd. https://doi.org/10.1016/j.compscitech.2010.01.010

29. Hu, J. J., Chao, W. C., Lee, P. Y., & Huang, C. H. (2012). Construction and characterization of an electrospun tubular scaffold for small-diameter tissue-engineered vascular grafts: A scaffold membrane approach. *Journal of the Mechanical Behavior of Biomedical Materials*, *13*, 140–155. https://doi.org/10.1016/j.jmbbm.2012.04.013

30. Duan, Y., Kalluri, L., Satpathy, M., & Duan, Y. (2021). Effect of Electrospinning Parameters on the Fiber Diameter and Morphology of PLGA Nanofibers. *Dental Oral Biology and Craniofacial Research*, 1–7. https://doi.org/10.31487/j.dobcr.2021.02.04

31. Xu, Y., Zou, L., Lu, H., & Kang, T. (2017). Effect of different solvent systems on PHBV/PEO electrospun fibers. *RSC Advances*, *7*(7), 4000–4010. https://doi.org/10.1039/c6ra26783a

32. Milleret, V., Hefti, T., Hall, H., Vogel, V., & Eberli, D. (2012). Influence of the fiber diameter and surface roughness of electrospun vascular grafts on blood activation. *Acta Biomaterialia*, *8*(12), 4349–4356. https://doi.org/10.1016/j.actbio.2012.07.032

33. Ko, Y. G., Park, J. H., Lee, J. B., Oh, H. H., Park, W. H., Cho, D., & Kwon, O. H. (2016). Growth behavior of endothelial cells according to electrospun poly(D,L-lactic-co-glycolic acid) fiber diameter as a tissue engineering scaffold. *Tissue Engineering and Regenerative Medicine*, *13*(4), 343–351. https://doi.org/10.1007/s13770-016-0053-7

34. You, Y., Min, B. M., Lee, S. J., Lee, T. S., & Park, W. H. (2005). In vitro degradation behavior of electrospun polyglycolide, polylactide, and poly(lactide-co-glycolide). *Journal of Applied Polymer Science*, *95*(2), 193–200. https://doi.org/10.1002/app.21116

35. Herrero-Herrero, M., Gómez-Tejedor, J. A., & Vallés-Lluch, A. (2018). PLA/PCL electrospun membranes of tailored fibres diameter as drug delivery systems. *European Polymer Journal*, *99*, 445–455. https://doi.org/10.1016/j.eurpolymj.2017.12.045

36. Alfaro De Prá, M. A., Ribeiro-do-Valle, R. M., Maraschin, M., & Veleirinho, B. (2017). Effect of collector design on the morphological properties of polycaprolactone electrospun fibers. *Materials Letters* 193, 154–157. https://doi.org/10.1016/j.matlet.2017.01.102

37. Yuan, H., Zhou, Q., & Zhang, Y. (2017). Improving fiber alignment during electrospinning. Mehdi Afshari (Ed), *Electrospun Nanofibers*, Woodhead Publishing - Elsevier Inc., 125–147. https://doi.org/10.1016/B978-0-08-100907-9.00006-4

38. Robinson, A. J., Pérez-Nava, A., Ali, S. C., González-Campos, J. B., Holloway, J. L., & Cosgriff-Hernandez, E. M. (2021). Comparative analysis of fiber alignment methods in electrospinning. In *Matter* (Vol. 4, Issue 3, pp. 821–844). Cell Press. https://doi.org/10.1016/j.matt.2020.12.022

39. Konig, G., McAllister, T. N., Dusserre, N., Garrido, S. A., Iyican, C., Marini, A., Fiorillo, A., Avila, H., Wystrychowski, W., Zagalski, K., Maruszewski, M., Jones, A. L., Cierpka, L., de la Fuente, L. M., & L'Heureux, N. (2009). Mechanical properties of completely autologous human tissue engineered blood vessels compared to human saphenous vein and mammary artery. *Biomaterials* 30(8), 1542–1550. https://doi.org/10.1016/j.biomaterials.2008.11.011

40. Jin, X., Geng, X., Jia, L., Xu, Z., Ye, L., Gu, Y., … Feng, Z. G. (2019). Preparation of Small-Diameter Tissue-Engineered Vascular Grafts Electrospun from Heparin End-Capped PCL and Evaluation in a Rabbit Carotid Artery Replacement Model. *Macromolecular Bioscience* 19(8). https://doi.org/10.1002/mabi.201900114

41. Yu, Y. H., Lee, D., Hsu, Y. H., Chou, Y. C., Ueng, S. W. N., Chen, C. K., & Liu, S. J. (2020). A three-dimensional printed polycaprolactone scaffold combined with co-axially electrospun vancomycin/ceftazidime/bone morphological protein-2 sheath-core nanofibers for the repair of segmental bone defects during the masquelet procedure. *International Journal of Nanomedicine*, *15*, 913–925. https://doi.org/10.2147/IJN.S238478

42. Zhan, J., Xu, H., Zhong, Y., Wu, Q., & Liu, Z. (2020). Surface modification of patterned electrospun nanofibrous films via the adhesion of DOPA-bFGF and DOPA-ponericin G1 for skin wound healing. *Materials and Design*, *188*. https://doi.org/10.1016/j.matdes.2019.108432

43. Hua, Y., Su, Y., Zhang, H., Liu, N., Wang, Z., Gao, X., Gao, J., & Zheng, A. (2021). Poly(lactic-co-glycolic acid) microsphere production based on quality by design: a review. *Drug Delivery*, *28*(1), 1342–1355. https://doi.org/10.1080/10717544.2021.1943056

44. Ji Lee, E., Ho Lee, J., Cheol Shin, Y., Hwang, D.-G., Soo Kim, J., Seong Jin, O., Jin, L., Won Hong, S., & Han, D.-W. (2014). Graphene Oxide-decorated PLGA/Collagen Hybrid Fiber Sheets for Application to Tissue Engineering Scaffolds. In *Biomater. Res* (Vol. 18, Issue 1).

45. Oztemur, J., Ozdemir, S., & Yalcin-Enis, I. (2022). Effect of blending ratio on morphological, chemical, and thermal characteristics of PLA/PCL and PLLA/PCL electrospun fibrous webs. *International Journal of Polymeric Materials and Polymeric Biomaterials*. https://doi.org/10.1080/00914037.2022.2090356

46. Mehrasa, M., Asadollahi, M. A., Ghaedi, K., Salehi, H., & Arpanaei, A. (2015). Electrospun aligned PLGA and PLGA/gelatin nanofibers embedded with silica nanoparticles for tissue engineering. *International Journal of Biological Macromolecules*, *79*, 687–695. https://doi.org/10.1016/j.ijbiomac.2015.05.050

47. Zamani, F., Latifi, M., Amani-Tehran, M., & Shokrgozar, M. A. (2013). Effects of PLGA nanofibrous scaffolds structure on nerve cell directional proliferation and morphology. *Fibers and Polymers*, *14*(5), 698–702. https://doi.org/10.1007/s12221-013-0698-y

48. Nath, S. D., Son, S., Sadiasa, A., Min, Y. K., & Lee, B. T. (2013). Preparation and characterization of PLGA microspheres by the electrospraying method for delivering simvastatin for bone regeneration. *International Journal of Pharmaceutics*, *443*(1–2), 87–94. https://doi.org/10.1016/j.ijpharm.2012.12.037

49. Silva, A. T. C. R., Cardoso, B. C. O., Silva, M. E. S. R. e, Freitas, R. F. S., & Sousa, R. G. (2015). Synthesis, Characterization, and Study of PLGA Copolymer *in Vitro* Degradation. *Journal of Biomaterials and Nanobiotechnology*, *06*(01), 8–19. https://doi.org/10.4236/jbnb.2015.61002

50. Masaeli, R., Kashi, T. S. J., Dinarvand, R., Tahriri, M., Rakhshan, V., & Esfandyari-Manesh, M. (2016). Preparation, Characterization and Evaluation of Drug Release Properties of Simvastatin-loaded PLGA Microspheres. In *Shaheed Beheshti University of Medical Sciences and Health Services Iranian Journal of Pharmaceutical Research*.

51. Enis, I. Y., Vojtech, J., & Sadikoglu, T. G. (2017). Alternative solvent systems for polycaprolactone nanowebs via electrospinning. *Journal of Industrial Textiles*, *47*(1), 57–70. https://doi.org/10.1177/1528083716634032

52. Hasan, M. A., Zaki, M. I., & Pasupulety, L. (2002). *Oxide-catalyzed conversion of acetic acid into acetone: an FTIR spectroscopic investigation*.

53. Oztemur, J., & Yalcin-Enis, I. (2021). Development of biodegradable webs of PLA/PCL blends prepared via electrospinning: Morphological, chemical, and thermal characterization. *Journal of Biomedical Materials Research - Part B Applied Biomaterials*, *109*(11), 1844–1856. https://doi.org/10.1002/jbm.b.34846

54. Hadjizadeh, A., Ajji, A., & Bureau, M. N. (2011). Nano/micro electro-spun polyethylene terephthalate fibrous mat preparation and characterization. *Journal of the Mechanical Behavior of Biomedical Materials*, *4*(3), 340–351. https://doi.org/10.1016/j.jmbbm.2010.10.014

55. Helling, A. L., Viswanathan, P., Cheliotis, K. S., Mobasseri, S. A., Yang, Y., El Haj, A. J., & Watt, F. M. (2019). Dynamic Culture Substrates That Mimic the Topography of the Epidermal-Dermal Junction. *Tissue Engineering - Part A*, *25*(3–4), 214–223. https://doi.org/10.1089/ten.tea.2018.0125

56. Sechi, M., Vanna, S., Roggio, A. M., Siliani, Massimo, P., Salvatore, M., & Mariani, A. (2012). Development of novel cationic chitosan- and anionic alginate–coated poly(D,L-lactide-co-glycolide) nanoparticles for controlled release and light protection of resveratrol. *International Journal of Nanomedicine*,5501-5516. https://doi.org/10.2147/IJN.S36684

57. Vasita, R., Mani, G., Agrawal, C. M., & Katti, D. S. (2010). Surface hydrophilization of electrospun PLGA micro-/nano-fibers by blending with Pluronic® F-108. *Polymer*, *51*(16), 3706–3714. https://doi.org/10.1016/j.polymer.2010.05.048

58. Cohn, D., & Hotovely Salomon, A. (2005). Designing biodegradable multiblock PCL/PLA thermoplastic elastomers. *Biomaterials*, *26*(15), 2297–2305. https://doi.org/10.1016/j.biomaterials.2004.07.052

59. Park, P. I. P., & Jonnalagadda, S. (2006). Predictors of glass transition in the biodegradable polylactide and poly-lactide-co-glycolide polymers. *Journal of Applied Polymer Science*, *100*(3), 1983–1987. https://doi.org/10.1002/app.22135

60. Peng, Z., Ye, L., & Ade, H. (2022). Understanding, quantifying, and controlling the molecular ordering of semiconducting polymers: From novices to experts and amorphous to perfect crystals. In *Materials Horizons* (Vol. 9, Issue 2, pp. 577–606). Royal Society of Chemistry. https://doi.org/10.1039/d0mh00837k

61. Yalcin Enis, I., Horakova, J., Gok Sadikoglu, T., Novak, O., & Lukas, D. (2017). Mechanical investigation of bilayer vascular grafts electrospun from aliphatic polyesters. *Polymers for Advanced Technologies* 28(2), 201–213. https://doi.org/10.1002/pat.3875

62. Wu, H., Fan, J., Chu, C. C., & Wu, J. (2010). Electrospinning of small diameter 3-D nanofibrous tubular scaffolds with controllable nanofiber orientations for vascular grafts. *Journal of Materials Science: Materials in Medicine*, *21*(12), 3207–3215. https://doi.org/10.1007/s10856-010-4164-8

63. Nezarati, R. M., Eifert, M. B., Dempsey, D. K., & Cosgriff-Hernandez, E. (2015). Electrospun vascular grafts with improved compliance matching to native vessels. *Journal of Biomedical Materials Research - Part B Applied Biomaterials* 103(2), 313–323. https://doi.org/10.1002/jbm.b.33201

64. Rodriguez-Soto, M. A., Suarez, N. A., Riveros, A., Garcia-Brand, A. J., Munoz-Camargo, C., Cruz, J. C., & Briceno, J. C. (2021). Mechanical characterization of novel vascular grafts: Approaching to the native vessel behavior. *2021 IEEE 2nd International Congress of Biomedical Engineering and Bioengineering, CI-IB and BI 2021*. https://doi.org/10.1109/CI-IBBI54220.2021.9626102

65. Tang, J., Bao, L., Li, X., Chen, L., & Hong, F. F. (2015). Potential of PVA-doped bacterial nano-cellulose tubular composites for artificial blood vessels. *Journal of Materials Chemistry B*, *3*(43), 8537–8547. https://doi.org/10.1039/c5tb01144b

66. Caves, J. M., Kumar, V. A., Martinez, A. W., Kim, J., Ripberger, C. M., Haller, C. A., & Chaikof, E. L. (2010). The use of microfiber composites of elastin-like protein matrix reinforced with synthetic collagen in the design of vascular grafts. *Biomaterials*, *31*(27), 7175–7182. https://doi.org/10.1016/j.biomaterials.2010.05.014

67. Chaparro, F. J., Matusicky, M. E., Allen, M. J., & Lannutti, J. J. (2016). Biomimetic microstructural reorganization during suture retention strength evaluation of electrospun vascular scaffolds. *Journal of Biomedical Materials Research - Part B Applied Biomaterials*, *104*(8), 1525–1534. https://doi.org/10.1002/jbm.b.33493

68. Grasl, C., Stoiber, M., Röhrich, M., Moscato, F., Bergmeister, H., & Schima, H. (2021). Electrospinning of small diameter vascular grafts with preferential fiber directions and comparison of their mechanical behavior with native rat aortas. *Materials Science and Engineering C* 124. https://doi.org/10.1016/j.msec.2021.112085

69. Ercolani, E., del Gaudio, C., & Bianco, A. (2015). Vascular tissue engineering of small-diameter blood vessels: Reviewing the electrospinning approach. *Journal of Tissue Engineering and Regenerative Medicine* 9(8), 861–888. https://doi.org/10.1002/term.1697